



Multiple Nonlinear Optical Response of Gold Decorated-Reduced Graphene Oxide-Nanocomposite for Photonic Applications

Research Article

Sudhakara Reddy Bongu¹, Prem B. Bisht^{1,*}, Tran V. Thu² and Adarsh Sandhu²

¹Department of Physics, Indian Institute of Technology Madras, Chennai 600036, India

²EIIRIS, Toyohashi University of Technology, 1-1 Hibarigaoka, Tempaku, Toyohashi 441-8580 Japan

*Corresponding author: bisht@iitm.ac.in

Abstract. Multiple *nonlinear optical* (NLO) responses of gold nanoparticles-grafted reduced graphene oxide (Au-rGO) nanocomposite have been studied with open aperture Z-scan setup. The nanocomposite shows the effect of *saturable absorption* (SA) at lower intensity that flips to *reverse saturable absorption* (RSA) on increasing the input irradiance. The results have been explained on the basis of the Pauli-blocking and multiphoton absorption. The NLO response of the material has been compared with the electronic diode characteristics. The simulations of the NLO responses of the nanocomposite have been done by varying saturation intensity and two-photon absorption coefficient of the material.

Keywords. Graphene, gold nanoparticles; Saturable absorption; Two photon absorption; Diode

PACS. 42.65.Re; 42.70.Mp; 78.67.Wj; 81.05.ue

Received: February 15, 2015

Accepted: September 26, 2015

Copyright © 2015 Sudhakara Reddy Bongu, Prem B. Bisht, Tran V. Thu and Adarsh Sandhu. *This is an open access article distributed under the Creative Commons Attribution License, which permits unrestricted use, distribution, and reproduction in any medium, provided the original work is properly cited.*

1. Introduction

Graphene composites can be used for wide range applications in photonics and optics due to their near-zero band gap nature [1]. Owing to the Pauli-blocking, the saturation of graphene absorption at strong pump excitations lead to the phenomenon of SA in graphene. It has been used as a passive modelocker for ultrafast pulse generation [2]. Multiphoton or excited-state

absorption, or the nonlinear scattering result in the broad-band optical limiting properties of the graphene composites [3]. In recent years, the broad band NLO responses of graphene composites have been utilized in opto-electronic device applications. The normal electronic diode action from the different NLO materials have been predicted [4] and observed [5]. The theoretical analysis has been done based on the switching from SA to *reverse saturable absorption* (RSA) of the graphene oxide to design all-optical femtosecond logic gates [6].

On the other hand, nanoparticles of metals such as silver and gold exhibit the *localized surface plasmon resonances* (LSPRs) in visible region [7]. The LSPRs bands can be tuned by varying the size, shape of the nanoparticles and the surrounding medium. The size and shape dependent NLO of metal nanoparticles have been reported [8]. The ZnO hosted gold nanoparticles films have been found to show the mode-locking [9]. The metal nanoparticles-grafted graphene composites shows an enhanced and multiple NLO responses than that bare graphene [10].

In view of the above, we performed the *open aperture* (OA) Z-scan experiments on gold nanoparticles-grafted reduced graphene oxide (Au-rGO) nanocomposites. The results have been compared with the function of an electronic diode. Simulations have been done for various values of the saturation intensity and two-photon absorption coefficient of the compound to understand the diode action of the compound for all optical devices.

2. Experimental

2.1 Sample Preparation and Characterization

Z-80 grade graphite flakes were provided by Ito Kokuen Co., Ltd. Gold (III) chloride solution (30 wt%) was purchased from Sigma-Aldrich. Sodium hydroxide and trisodium citrate dehydrate were obtained from Kanto Chemical Co., Inc. Deionized water was used as solvent for the experiment.

Graphene oxide (GO) was synthesized using a modified Hummer's method [11]. Au-rGO hybrids were synthesized by citrate reduction method. GO solution (2.5 mg in 5 ml H₂O), gold (III) chloride solution (~5.0 mg Au in 5 ml H₂O), sodium hydroxide 0.1 M (5 ml), were brought to boil in a three-necked-flask. Trisodium citrate dihydrate solution (1 g in 15 ml H₂O) was added into the flask at once, and the boiling solution was kept stirring at 500 rpm for 1 hour. To obtain the Au-rGO powder the solution was filtrated, washed several times and dried. UV-vis absorption spectra were carried out with the Jasco, V-570 dual beam spectrometer. Raman spectrum was recorded with a Jobin Yvon model HR-800 equipped with a He-Ne laser (632.8 nm). Electron microscopic imaging was done with the Hitachi S-4800 *field-emission scanning electron microscope* (FESEM).

2.2 Z-scan Experiment

The NLO responses of Au-rGO composite was measured using an *open aperture* (OA) Z-scan experiment (Figure 1). The second harmonic (532 nm, 30 ps) of the Nd: YAG laser was used as the excitation wavelength. The sample was taken in to 1mm thick glass cell and scanned over the focal plane of 50 mm lens. The transmitted light from the sample was collected at far field

by a large aperture double convex lens and was detected by the photodiode (Becker and Hickl, PDI 400). Data were collected with the help of a home built data processing system by using a LabView software in a PC.

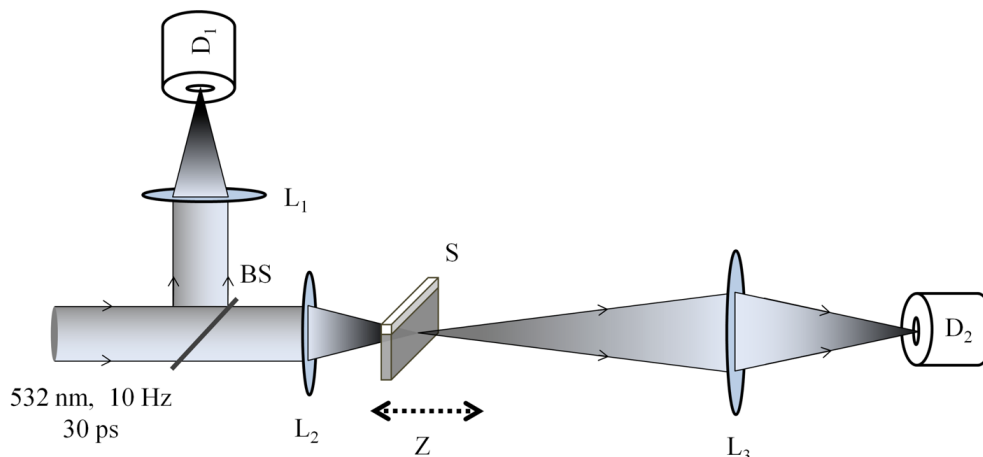


Figure 1. OA Z-scan experimental setup. BS is the beam splitter, L_1 , L_2 and L_3 are the double convex lenses. S is the sample, D_1 and D_2 are the reference and signal detectors, respectively.

3. Theoretical Aspects

The case at simultaneous occurrence of SA and RSA behavior, the intensity dependent absorption coefficient $\alpha(I)$ is given by [10]

$$\alpha(I) = \frac{\alpha_0}{1 + \frac{I}{I_s}} + \beta_{2PA} I, \quad (1)$$

where I_s , is the saturation intensity, I ($= \frac{I_0}{1+x^2}$) is the input irradiance and I_0 is the input irradiance at the focus. $x = \frac{z}{z_0}$, z_0 is the Rayleigh range; α_0 and β_{2PA} are the linear and two photon absorption coefficients, respectively. The total nonlinear absorption coefficient (β) and the normalized transmittance are given by

$$\beta = \frac{\alpha(I) - \alpha_0}{I}, \quad (2)$$

$$T(I) = 1 - \frac{\beta I L_{\text{eff}}}{2}, \quad (3)$$

where L_{eff} is the effective path length of the sample.

4. Results and Discussion

4.1 Steady state Measurements

4.1.1 Absorption Analysis

Figure 2A shows the broad range wavelength absorption spectra of rGO and Au-rGO nanocomposites. The optical density for rGO increases monotonously towards shorter

wavelength. The additional band at 560 nm for Au-rGO nanocomposite corresponding to the LSPRs bands of gold nanoparticles. The arrow indicates the pump wavelength (532 nm) for Z-scan experiment.

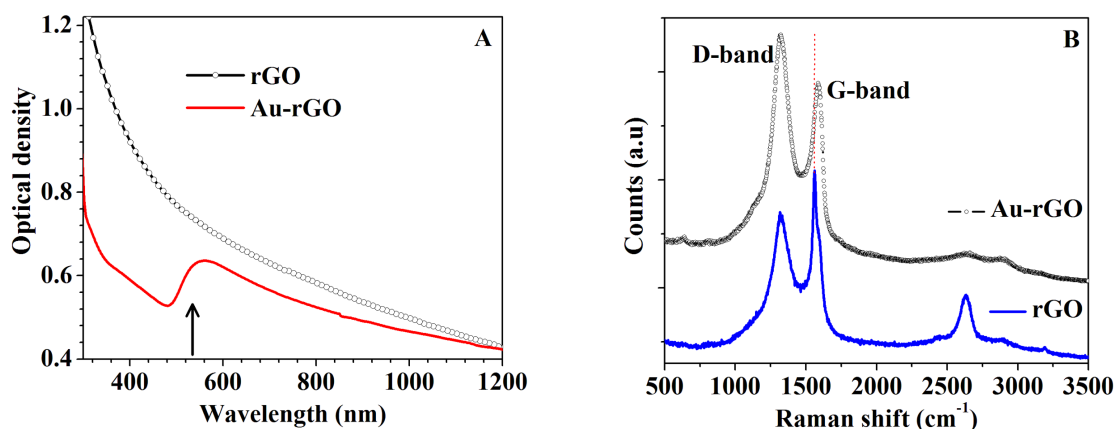


Figure 2. Absorption (panel A) and Raman (panel B) spectra of GO and Au-rGO. Arrow in absorption spectra indicates the pump wavelength (532 nm) for Z-scan experiment.

4.1.2 Raman Analysis

The Raman spectra of rGO and Au-rGO are shown in Figure 2B. The characteristic D-band and G-band of rGO were observed at 1316 cm^{-1} and 1560 cm^{-1} , respectively. Au-rGO exhibits its D and G-bands at 1317 cm^{-1} and 1586 cm^{-1} , respectively. The 26 cm^{-1} red shift of the G-band in Au-rGO is due to the electron transfer between adsorbed AuNPs and rGO flakes [12]. The ratio of intensities of D-band (I_D) to G band (I_G) of the rGO and Au-rGO, respectively are 0.82 and 1.22. The small increase in intensity of D-band for Au-rGO can be attributed to the surface enhanced Raman scattering by AuNPs adsorbed on the rGO flakes.

4.1.3 FESEM Analysis

Figure 3 shows the FESEM image of Au-rGO nanocomposite. The estimated mean particles size of the AuNPs decorated on rGO flakes are 20 nm.

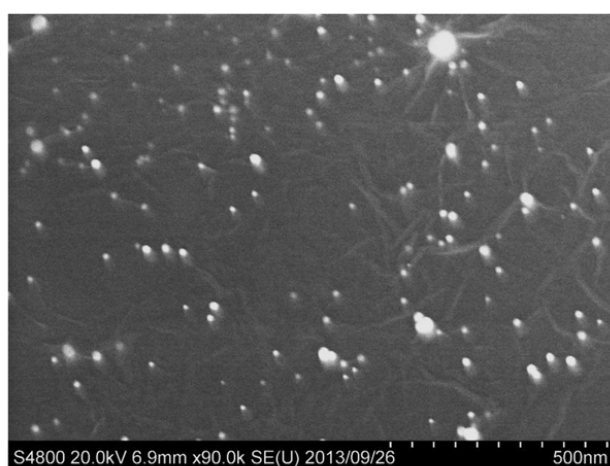


Figure 3. FESEM images of AuNPs decorated on rGO flakes.

4.2 Nonlinear Transmittance

The open aperture Z-scan profiles of Au-rGO are shown in Figure 5. The nanocomposite exhibits the increase in the transmittance with input intensity (i.e., the effect of SA) at lower irradiance regime. The mechanism for the observed SA can be explained based on the Pauli-Blocking. Due to the zero band gap nature of graphene, the photo-excitation takes place from valence band to the conduction band even for excitation by low photon energy [10, 13]. This results in the creation of a hole at the valence band. The photo-generated carriers accumulated near the conduction and valence bands by several intraband processes (carrier-carrier scattering and carrier-phonon coupling) on a sub ps time scale. Finally, relaxation takes place through the intraband phonon scattering and electron-hole recombination on a timescale of approximately 2 ps. [13]. The photo excitation and relaxation process is shown in Figure 4. Further increases in the input irradiance increase the number of carriers in the conduction band. The consequence of the Pauli exclusive principle prevents the further interband transition and is known as Pauli blocking. It is due to the Pauli blocking, on further increase of incident irradiance, that the transmittance increases resulting in the effect of SA.

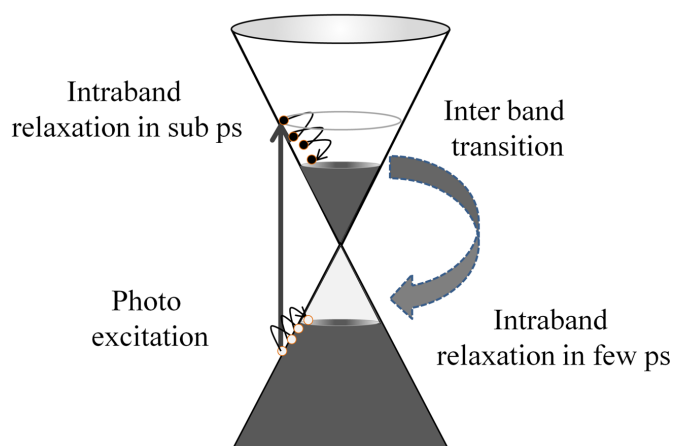


Figure 4. Photo excitation and relaxation process in graphene

On further increasing the input irradiance, the profiles shows a dip at the focus that is known as the *reverse saturable absorption* (RSA). At higher input irradiance, the profile shows complete RSA behavior. At higher pump photon densities the Pauli-Blocking can be overcome by the further interband transition due to two or multiphoton absorption. It decreases the transmitted light intensity. Other than SA effect [9], the plasmonic nanoparticles can induce the extra polarization to the rGO by LSPRs due to excitation at the near plasmonic band (2.2 eV) in low intensity regime. At high input intensity the 2PA (4.7 eV) from AuNPs also contributes to the effective decrease in the transmittance [14]. By using equation (1) and (3), the estimated saturation intensity I_S and two photon absorption coefficient (β_{2PA}) of the nanocomposite are $3.4 \times 10^{13} \text{ W/m}^2$ and $4.6 \times 10^{-12} \text{ m/W}$, respectively.

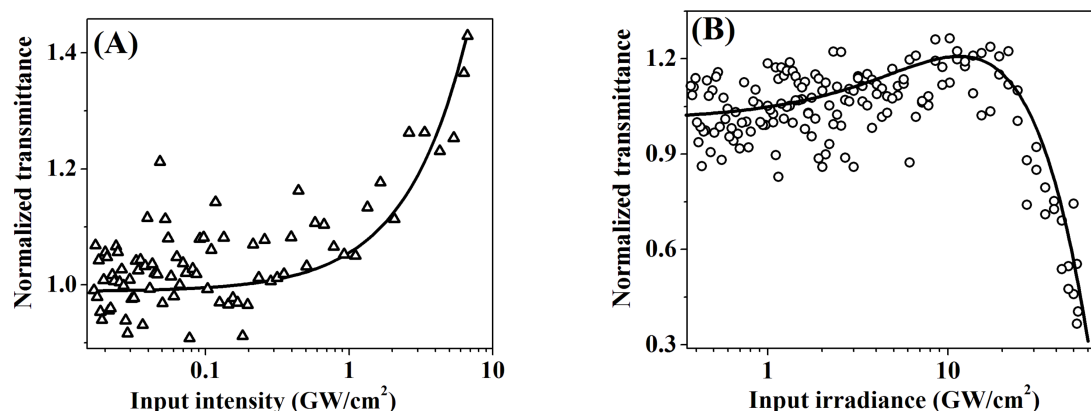


Figure 5. Obtained plots of normalized transmittance vs input irradiance from the OA Z scan profiles of Au-rGO. Solid lines are theoretical fit to the experimental data using equation (3) (Panel A and B).

4.3 Comparison with Electronic Diode Action and Theoretical Simulations

Diode is a non-linear semiconductor electronic device, generally used in all electronic circuits. It allows the current in one direction and restrict in other. The ideal I_c - V characteristic of the basic diode is given in Figure 6A, shows the response of flow of current in the device with respect to the input voltage. The knee voltage indicates the rapid increase in the current at particular input voltage in forward bias. The damage voltage of the diode in the reverse bias is known as break down voltage. The special case of the normal diode is Zener diode, it allows the current in the reverse bias also.

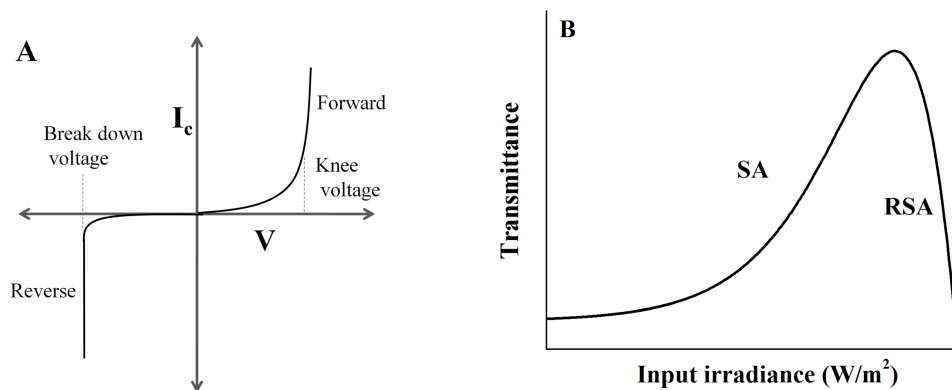


Figure 6. Panels (A), the current-voltage characteristic curve for the electronic diode. Panel (B) gives the corresponding to the NLO response of the nanocomposite.

The NLO response of Au-rGO nanocomposite can be compared with the normal electronic diode (Figure 6B). Increase or decrease in the transmittance of NLO material can be considered as a flow of current in positive and negative direction of electronic diode, while input intensity is analogues to the input voltage. The nanocomposite exhibits the increase in the transmittance at low input irradiance regime and decreases at high input pump irradiance. In contrast to the p-n diodes, irrespective of the direction of excitation of the sample, this nanocomposite can act as an intensity dependent forward and reverse bias diode. Especially this response is similar

to the switching diode action with multiple stop point. Here, the diode will resist at particular intensity and turn in to a closed switch to conduct the circuit. The graphene based composites with plasmonic nanoparticles have been reported to shows the enhanced NLO response [10]. The combinations with other nanocomposites can make an efficient NLO diode.

The simulations (Figure 7) were done based on the equation (3) at varying saturation intensity (constant β_{2PA}) and nonlinear absorption coefficient (constant I_s) for obtained the optimal conditions of combined NLO effect in the nanocomposites.

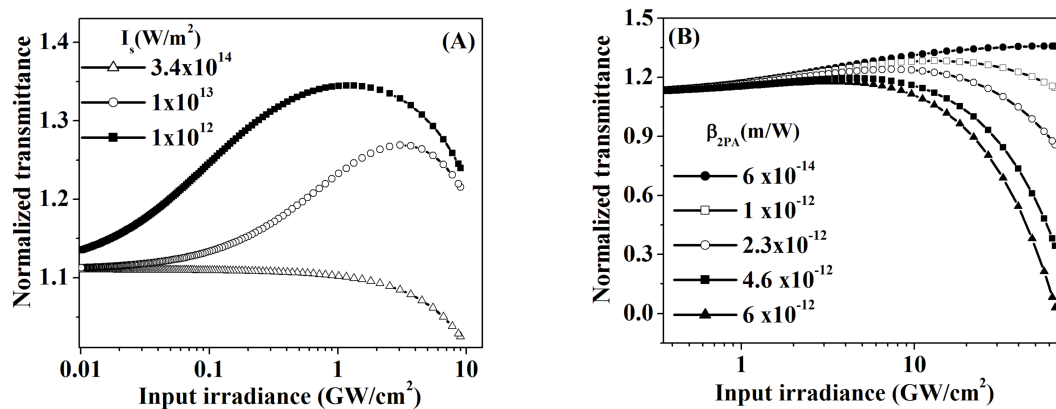


Figure 7. Panels (A) and (B) give theoretical simulations of transmittance of a nanocomposite for different I_s (at constant $\beta_{2PA} = 4.6 \times 10^{12}$ m/W) values β_{2PA} (at constant $I_s = 3.4 \times 10^{13}$ W/m²) and, respectively.

5. Conclusions

The NLO responses of Au-rGO nanocomposite have been studied with OA Z-scan setup under ps excitation at 532 nm. The system shows SA behavior at lower input irradiance and flips to RSA at high irradiance. Comparison has been made with electronic diode action. Simulations were done for better NLO performance of the nanocomposite. Multiple and enhanced NLO responses of metal nanoparticles grafted graphene has been proposed to be a better candidate for the opto-electronic devices.

Acknowledgements

We thank CSIR, New Delhi for financial assistance.

Competing Interests

The authors declare that they have no competing interests.

Authors' Contributions

All the authors contributed significantly in writing this article. The authors read and approved the final manuscript.

References

- [1] F. Bonaccorso, Z. Sun, T. Hasan and A.C. Ferrari, *Nat. Photon.* **4** (2010), 611–622.
- [2] Z. Sun, T. Hasan, F. Torrisi, D. Popa, G. Privitera, F. Wang, F. Bonaccorso, D.M. Basko and A.C. Ferrari, *ACS Nano.* **4** (2010), 803–810.
- [3] S. Husaini, J.E. Slagle, J.M. Murray, S. Guha, L.P. Gonzalez and R.G. Bedford, *Applied Physics Letters* **102** (2013), 191112–191116.
- [4] C.G. Treviño-Palacios, G.I. Stegeman and P. Baldi, *Optics Letters* **21** (1996), 1442–1444.
- [5] R. Philip, M. Anija, C.S. Yelleswarapu and D.V.G.L.N. Rao, *Applied Physics Letters* **91** (2007), 141118–141121.
- [6] S. Roy and C. Yadav, *Applied Physics Letters* **103** (2013), 241113–241117.
- [7] K.L. Kelly, E. Coronado, L.L. Zhao and G.C. Schatz, *The Journal of Physical Chemistry B* **107** (2002), 668–677.
- [8] O. Muller, S. Dengler, G. Ritt and B. Eberle, *Applied Optics* **52** (2013), 139–149.
- [9] S.A. Ali, P.B. Bisht, B.S. Kalanoor, A. Patra and S. Kasiviswanathan, *Journal of the Optical Society of America B* **30** (2013), 2226–2232.
- [10] S.R. Bongu, P.B. Bisht, R.C.K. Nambodiri, P. Nayak, S. Ramaprabhu, T.J. Kelly, C. Fallon and J.T. Costello, *Journal of Applied Physics* **116** (2014), 073101–073106.
- [11] T. Thu, P. Ko, N. Phuc and A. Sandhu, *Journal of Nanoparticle Research* **15** (2013), 1–13.
- [12] A.K. Manna and S.K. Pati, *Chemistry – An Asian Journal* **4** (2009), 855–860.
- [13] Q. Bao, H. Zhang, Y. Wang, Z. Ni, Y. Yan, Z.X. Shen, K.P. Loh and D.Y. Tang, *Advanced Functional Materials* **19** (2009), 3077–3083.
- [14] B. Anand, R. Podila, K. Lingam, S.R. Krishnan, S. Siva Sankara Sai, R. Philip and A.M. Rao, *Nano Letters* **13** (2013), 5771–5776.